Langmuir

Article

pubs.acs.org/Langmuir

Modeling Self-Assembly of Silica/Surfactant Mesostructures in the Templated Synthesis of Nanoporous Solids

Germán Pérez-Sánchez,[†] José R. B. Gomes,[‡] and Miguel Jorge*[,†,§]

[†]LSRE - Laboratory of Separation and Reaction Engineering - Associate Laboratory LSRE/LCM, Faculdade de Engenharia, Universidade do Porto, Rua Dr. Roberto Frias, 4200-465 Porto, Portugal

[‡]CICECO, Departamento de Química, Universidade de Aveiro, Campus Universitário de Santiago, 3810-193 Aveiro, Portugal

[§]Department of Chemical and Process Engineering, University of Strathclyde, 75 Montrose Street, Glasgow G1 1XJ, United Kingdom

Supporting Information

ABSTRACT: A novel coarse-grained (CG) model to study the self-assembly of silica/surfactant mesostructures during the synthesis of periodic mesoporous silica is reported. Molecular dynamics simulations of hexadecyltrimethylammonium bromide (also called cetyltrimethylammonium bromide, or CTAB) surfactants in water and in aqueous silicate solutions have been performed to understand micelle formation, micelle growth, and their size evolution during the synthesis of surfactant-templated mesoporous materials. Direct comparison of density profiles obtained for preassembled micelles employing an all-atom description, AA, with those calculated with the CG model has been carried out for checking the validity of the latter model. Good agreement between AA and CG approaches was found, demonstrating the potential of the CG approximation for modeling these highly complex systems. The micelle formation and micelle fusion/fission processes were analyzed after performing long CG simulations for surfactant and ionized silica−surfactant aqueous solutions. We observed the formation of rodlike micelles in the case of silica−surfactant solutions, while spherical micelles were stable under the same conditions for the CTAB+H_2O system. This demonstrates that the interaction of anionic silicates with cationic surfactants promotes a sphere-to-rod transition in surfactant solutions, a key step in the synthesis of nanoporous silica materials.

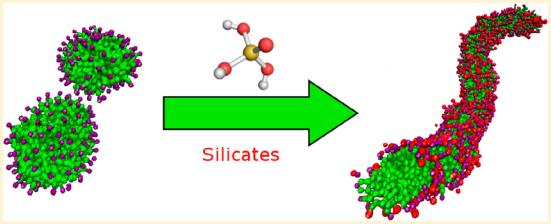

1. INTRODUCTION

The amphiphilic character of surfactant molecules (hydrophobic tail and hydrophilic head) promotes a spontaneous self-assembly in aqueous solution into a variety of different aggregates, including micelles, rods, vesicles, and liquid crystals. The shape and size of these aggregates depend on chemical and environmental conditions like temperature, presence of counterions, surfactant chain length, and concentration.[1] Cationic alkylammonium surfactants are among the most widely studied systems due to their applications as dispersants, detergents, and, more importantly for the present work, as templates for the synthesis of nanoporous materials. The synthesis of periodic mesoporous silica (PMS) is based on the latter process, whereby a surfactant acts as a template.[2] PMS are well-known for their applications in engineering and chemistry, including shape-selective catalysis or selective adsorption, mainly because of their regular pore structure.[3] Despite having been studied for several years using both experimental[4−6] and theoretical[7−9] tools, many details of PMS formation mechanism are not yet fully understood, particularly during the early stages of the synthesis process. This lack of knowledge is all the more serious if we consider that the final material properties depend significantly on the early stages of the synthesis.[4] Indeed, although PMS offer the possibility to control the pore size by changing the synthesis conditions, a true a priori design of a material with a given set of desired properties is still an elusive goal.

The synthesis of PMS is conceptually simple, with silica condensing around a surfactant liquid crystal, which imparts the desired pore geometry and is then removed, normally by calcination, to yield an ordered nanoporous silicon oxide material. However, the physicochemical mechanisms by which the material is formed are rather complex, involving hydrophobic effects, solvation, chemical reactions, and phase equilibrium, all taking place simultaneously. This makes it very difficult to probe the entire process using experimental techniques, and suggests that molecular simulation may be an extremely useful tool to further understand PMS synthesis. However, relatively few simulation studies aiming to model the synthesis of PMS materials have been carried out so far. Siperstein and Gubbins[8,10] performed Monte Carlo simulations of a lattice model to explore the phase diagram of silica−surfactant−solvent systems, which showed qualitative agreement with experimental observations. Their model was later extended to deal with hybrid organic−inorganic precursors.[11,12] The main drawback of their approach was the inability of the model to explain the molecular-level details that govern silica/

Received: November 20, 2012
Revised: January 22, 2013
Published: January 23, 2013

   dx.doi.org/10.1021/la3046274 | *Langmuir* 2013, 29, 2387−2396

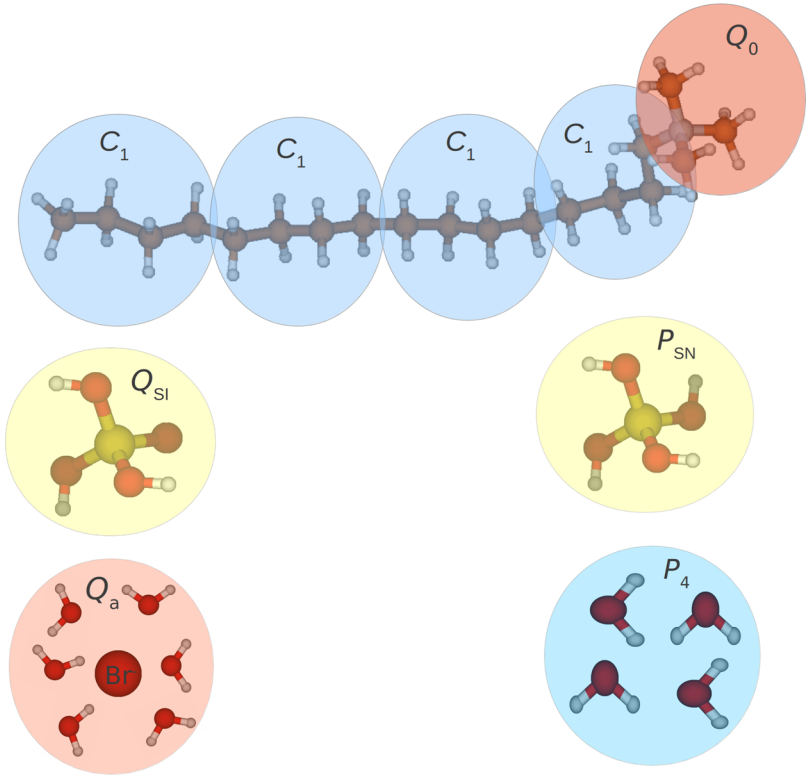

Figure 1. Schematic diagram of the coarse-graining procedure employed in this work for the CTA^+ surfactant; neutral and anionic silicate monomers; solvated bromide ion (surrounded by six water molecules), and water (representing four real water molecules). The labels correspond to MARTINI bead types (except for the new silicate beads).

surfactant aggregate formation, relying instead on an assumed effective interaction between those species. Schumacher et al.[13] described the condensation reactions between silicates at the micelle surface, albeit with a much simplified model to ensure computational tractability. Once again, their model relied on an assumed effective attraction between silicates and micelles.

Recently, our group has used a different approach, based on atomistic molecular dynamics (MD) simulations of the initial stages of PMS synthesis.[14,15] The surfactant model was first validated by carrying out simulations of surfactant/water solutions.[16,17] Subsequently, several PMS synthesis solutions, including silicates, surfactants, water and counterions, and representing different stages of the synthesis process, were carried out. It was demonstrated that silica monomers (monosilicic acid molecules) adsorb strongly on the surface of the micelles, replacing bromide counterions, and promote the growth of initially small spherical aggregates.[14] As the degree of silica condensation increases, multicharged silicate oligomers start to interact with more than one micelle at the same time, in what could constitute the first steps of supramicelle aggregation.[15] Unfortunately, atomistic simulations are currently limited to about 100 000 atoms and a time scale of tens of nanoseconds due to high computational requirements. As such, it was necessary to focus on systems with a relatively high concentration and a small-chain surfactant. Importantly, on this time scale, it is not possible to study in detail the evolution of micelle fusion/fission processes or to observe sphere-to-rod transitions, which are crucial steps in PMS synthesis. In this work, we attempt to circumvent this limitation by performing much longer simulations of PMS synthesis solutions using a coarse-grained (CG) model. By significantly reducing the number of interaction centers in each molecule and speeding up the dynamics, CG models are able to probe much longer time scales than is possible using atomistic models, and have recently provided new insight into sphere-to-rod transitions in aqueous solutions of ammonium surfactants.[18] We started from the MARTINI force field developed by Marrink and co-workers,[19,20] which is able to represent the essential characteristics of several different molecules, including phospholipid surfactants. This model was applied successfully in different surfactant aqueous solutions[18,21,22] where the CG procedure was validated by comparing atomistic and CG simulations. In this work, we focused our attention on aqueous solutions of hexadecyltrimethylammonium surfactant (also called cetyltrimethylammonium, and denoted as CTA^+) with bromide counterions (the ion pair is hereafter denoted as CTAB) and neutral, $Si(OH)_4$, or anionic, $Si(OH)_3O^-$, silicate monomers (following our previous nomenclature,[15] the neutral silica monomer is denoted as SN while the anionic form is denoted as SI). These mixtures correspond to the most common starting synthesis conditions for PMS materials. Because there were no available interaction parameters for silicates in the MARTINI force field, we developed our own set of parameters following the original coarse-graining philosophy and validated them against atomistic MD simulations.

This paper is organized as follows. Section 2 shows the systems under study and describes the coarse-graining method and the computational details. Section 3 presents the main results and is divided into two parts: the first part describes the development of a CG model for surfactant/silicate solutions and validation against atomistic simulation results, while in the second part long CG simulations are performed to describe the formation and evolution of micelles during the PMS synthesis

dx.doi.org/10.1021/la3046274 | *Langmuir* 2013, 29, 2387−2396

process. Section 4 summarizes the main conclusions obtained in this work.

2. SIMULATION DETAILS

Two different types of MD simulations were performed in this work: simulations starting from individual preformed spherical micelles, for calibrating and validating the molecular models, and simulations starting from randomly arranged configurations to study the self-assembly of micelles in the presence of silica during the PMS synthesis process. The former were carried out with both all-atom (AA) and CG models, while the latter were performed only with the CG model in order to probe the long time scales necessary to observe rodlike micelle formation. All simulations were carried out with GROMACS 4.5.5[23−26] using a leapfrog algorithm[27] to integrate the equations of motion. The time step for the AA simulations was 2 fs, while for the CG runs it was 30 fs. The simulation box was always cubic with periodic boundary conditions in all directions of space. The temperature (T) was kept fixed at 298 K with the velocity-rescaling thermostat,[28] while the pressure was fixed at 1 bar, when necessary, using the Parrinello−Rahman barostat[29] for the AA case and the Berendsen pressure-coupling method[30] for the CG case.

The energy contributions in the potential energy function were bond stretching, angle bending, torsion, Lennard−Jones (LJ), and Coulombic terms. Bond lengths were constrained by the LINCS algorithm[31] in AA simulations. The atomistic models used here were the same as in our previous papers,[14,15,17] and detailed tables of parameters are provided in those publications. For the CTAB surfactant, we used parameters taken from the OPLS potential.[32] Although in a previous study[17] we showed that a united-atom description of the surfactant tails yielded a very good description of the properties of decyltrimethylammonium bromide with reduced computational cost relative to a fully atomistic description, we have chosen to use the more realistic AA model for validating the CG potential. The rigid SPC/E potential[33] was used to represent the water molecules, while silicates were represented by our own potential model,[14,15] which was based on data obtained from quantum mechanical calculations on several neutral and anionic silicates.[34−36] A shifted LJ potential was employed, where the energy decays smoothly to zero between 1.0 and 1.1 nm, while long-range electrostatic interactions were evaluated by a combination of particle mesh Ewald and a switching function (PME-Switch keyword in GROMACS) with a cutoff radius of 1.1 nm.

The CG procedure basically consisted of splitting each molecule into beads, depending on its physicochemical behavior, and then assigning one of the bead types proposed by Marrink and co-workers.[19,20] As mentioned in the Introduction, the CG model for cationic alkylammonium surfactants was recently successfully validated by Wu et al.[18] for dodecyltrimethylammonium bromide solutions. We have thus divided our CTA^+ molecule into five beads with four heavy atoms each (according to the philosophy of the MARTINI force field), where four of the beads correspond to alkyl groups and the last bead represents the hydrophilic head. We assigned the same bead types as Wu et al.,[18] namely, C_1 (nonpolar) type for alkyl beads and Q_0 (charged) type for the surfactant head, while bromide ions were described by a single charged Q_a (hydrogen-bond acceptor) bead. It is worth noting that the bromide CG bead implicitly contains six solvating water molecules, as prescribed by Marrink and co-workers[19,20] for the representation of simple monatomic ions in solution. Also according to the MARTINI force field, each CG water bead represents four atomistic water molecules. Each silicate monomer (neutral or anionic) was represented by a single CG bead. Since there are no available parameters in the literature for silicates, we have developed and validated our own CG model for these molecules (see section 3.1). A schematic representation of the coarse-graining procedure for all molecules can be seen in Figure 1. Following the procedure of Marrink and co-workers,[19,20] a shifted LJ energy function was used to describe nonbonded interactions, with parameters taken from the MARTINI 2.0 force field (a full interaction matrix is available in the original publication[20]). In the case of bonded interactions, a harmonic potential with an equilibrium bond length of 0.47 nm and stretching force constant of 1250 $kJ{\cdot}mol^{-1}{\cdot}nm^{-2}$ was used, while LJ interactions between bonded particles were not considered. The angle force term was 25 $kJ{\cdot}mol^{-1}$ with an equilibrium bond angle of 180° for the angle bending harmonic potential. van der Waals and electrostatic interaction potentials were computed with a cutoff radius of 1.2 nm, and the relative dielectric constant of the medium was fixed to 15.[20] It is worth noting that in all CG simulations it was necessary to add a concentration of 0.1 M of antifreeze particles, as prescribed by Marrink et al.,[19] to avoid unphysical freezing of the CG solvent during the simulations.

For the development and validation of the CG model starting from preformed micelles, we have considered three different aqueous solutions: (1) CTAB+H_2O; (2) CTAB+SN+H_2O; (3) CTA^++SI +H_2O. The first solution enabled us to validate the surfactant CG model, while solutions 2 and 3 formed the basis for the development of our CG model for neutral and anionic silicates, respectively. All simulations were carried out at concentrations well above the critical micelle concentration (cmc) for CTAB, ∼0.8 mM,[37−39] where it is well-known that micelles are formed experimentally. Preformed micelles were prepared using the PACKMOL[40] package, both in the AA and CG descriptions. This software packs a specified number of surfactant molecules in a spherical arrangement, and then randomly distributes solvent and counterions (in this case bromide and silicates) around the micelle. The AA version of the CTAB+H_2O solution contains a preassembled micelle of 100 CTAB ion pairs (corresponding to experimental estimates of the average aggregation number[41−47]) solvated with 50 000 H_2O molecules. This corresponds to 100 CTAB surfactants solvated with 12 500 H_2O particles in the CG version to maintain the same concentration (recall that each CG water bead corresponds to four real water molecules). In the case of surfactant +silicate solutions, we have two aqueous solutions of similar concentration, one with 100 CTAB ion pairs and 150 SN neutral silicate monomers and another one with 100 CTA^+ surfactants (i.e., without bromide) and 100 SI ionized silicate monomers (which in this case act as counterions), both solvated with 50 000 water molecules in the AA version and 12 500 in CG. After building the initial configuration, each run was first energy minimized, followed by short sequential equilibration runs in the NVT and in the NpT ensembles. After equilibration, MD production runs with a simulation time of 20 ns were carried out.

For the long CG simulations of silica/surfactant micelle formation, we prepared a set of configurations with 900 CTAB surfactants in the case of the CTAB+H_2O system and with 900 ionized surfactants CTA^+ plus 900 ionized silicate monomers for the CTA^++SI+H_2O system. In both systems, two mixtures were prepared with 125 000 and 250 000 CG water particles, yielding solutions with approximately 0.1 and 0.05 M surfactant concentrations, respectively. We also considered solutions with different ion concentrations and with different ratios of neutral to ionized silicates (see section 3.2 for details). Note that, contrary to the simulations for the development and validation of the CG model, the initial configurations in the longer CG simulations were built by randomly dispersing all components of the solution within the simulation box using PACKMOL. This was followed by energy minimization and quick NVT and NpT equilibration runs. The production runs were as long as 7.6 μs. It is important to notice that, apart from allowing for the use of a larger time step in MD, the process of coarse-graining also intrinsically speeds up the dynamics by a factor between 2 and 10, depending on the nature of the system.[19] However, because in this paper we are not concerned with the absolute values of dynamical properties, the time that we report in our results is the simulation time (i.e., simply the number of frames multiplied by the time step). Following Marrink et al.,[19] it is possible to obtain a reasonable estimate of the effective time (closer to the real time scale) by multiplying the simulation time by 4.

Individual micellar aggregates in each simulation were identified using an in-house code based on the Hoshen−Kopelman cluster-counting algorithm.[48] In the atomistic simulations, following our previous work,[17] two surfactant molecules were considered to belong to the same aggregate if any of their last four tail carbon atoms were

dx.doi.org/10.1021/la3046274 | Langmuir 2013, 29, 2387−2396

separated by no more than 0.64 nm (corresponding to the first minimum in the radial distribution function between tail carbon atoms). This criterion had to be adapted for the CG model due to the reduction in atomistic detail: based on the same principles, two surfactants belonged to the same aggregate if their last tail beads (equivalent to four ethyl/methyl groups) were located at a distance below 1.2 nm. This criterion was tested by comparing results of the cluster-counting procedure with visual inspection of selected simulation snapshots.

3. RESULTS AND DISCUSSION

In the first part of this section (section 3.1) we begin by presenting the results of AA and CG simulations starting from preassembled micelles with the aim of developing and validating a new CG model for silicates. In the second part (section 3.2), results from long CG simulations starting from random initial configurations will be displayed, comparing the micelle formation and evolution in solutions with and without silicates.

3.1. CG Model Validation for Silica–Surfactant Solutions. Because silicic acid is very unstable and reacts very quickly in solution to form polymeric silicates,[49] there are no pure-fluid experimental properties (e.g., density, enthalpy of vaporization, etc.) that can be used to calibrate the model. Therefore, following previous coarse-graining strategies,[18−20] we have developed our model based on a comparison between AA and CG simulation results for the structure of preformed spherical micelles of the same size, particularly by comparing the density profiles measured from the center of mass (COM) of the micelle. As we will see below, this turns out to be a rather stringent test for our parameter set for CG silicates.

We begin by testing the capability of the CG representation of the surfactant by comparing density profiles for a single CTAB micelle in water, shown in Figure 2. In order to identify

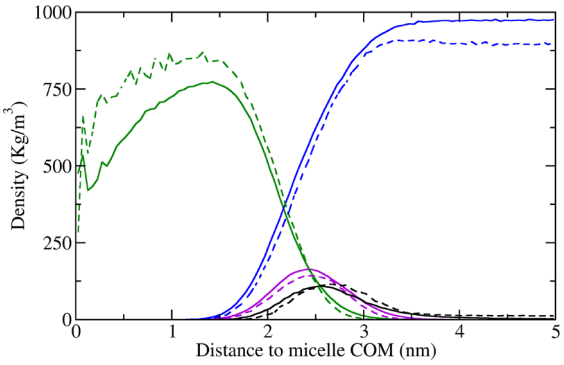

Figure 2. Comparison between all-atom and coarse-grained density profiles for the CTAB+H_2O system measured from the center of mass of a single preformed micelle. Tail atoms are shown in green, head atoms in purple, water in blue, and bromide ions in black. Solid and dashed lines represent the AA and the CG models, respectively.

the different parts of each molecule in the density plots, we have assigned the nitrogen and the surrounding three methyl groups as part of the headgroup in the case of the AA surfactant, and the corresponding Q_0 bead for the CG model, both shown in purple. The rest of the surfactant molecule is assigned to the tail, shown in green, the bromide ions are shown in black, while the solvent is always shown in blue. The profiles in Figure 2 show the typical structure of a cationic surfactant micelle; the hydrophobic core is composed of only tail atoms, which are separated from the solvent by a well-defined layer of headgroup atoms. It can also be seen how the bromide ions arrange themselves close to the surface of the micelle on the solvent side of the headgroup layer, forming a rather diffuse counterion Stern layer to balance the positive charge of the surfactant heads. It is important to remember that the bromide ions were placed in random positions surrounding the micelle surface at the beginning of the simulations. Also, in Figure 2 we can see how the solvent penetrates slightly into the micelle surface, as expected for this type of surfactant.[17,50] The profiles for AA and CG simulations, plotted in straight and dotted lines, respectively, show excellent agreement in the relative location of each type of atom. The average value of the bulk water density is slightly underestimated in the CG model (a well-known consequence of the coarse-graining procedure[19,20]), while the density of the hydrophobic core is slightly overestimated. The important observation, however, is that both AA and CG micelles have analogous structures, thus showing that the CG model represents very well the behavior of CTAB surfactants in aqueous solution, which is in agreement with previous conclusions by Wu et al.[18]

For modeling silicates, our initial approach was to consider only CG bead types already included in the MARTINI force field. Thus, ionized silicates were tentatively represented by one bead of the Q_{da} type (the subscript "da" stands for donor–acceptor hydrogen-bond character[19,20]), while neutral silicates were represented by a polar P_5 bead type. In Figure 3, we show

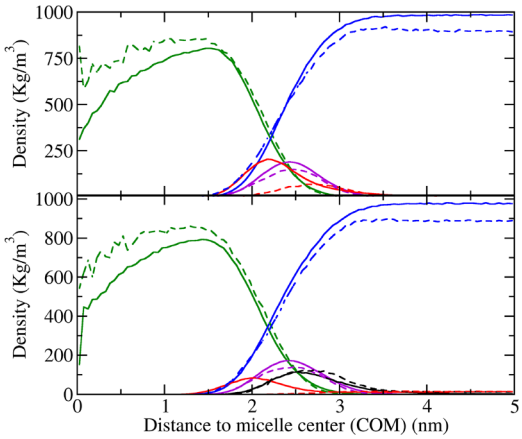

Figure 3. Density profiles for all-atom (solid lines) and coarse-grained (dashed lines) models in (top) the CTA^++SI+H_2O system using a Q_{da} CG bead for anionic silicates; (bottom) the CTAB+SN+H_2O system using a P_5 CG bead for neutral silicates. Tail atoms are shown in green, head atoms in purple, water in blue, bromide ions in black, and silicates in red.

the results for CTA^++SI+H_2O and CTAB+SN+H_2O, where the silicate density profile is shown in red. As for the CTAB+H_2O system, the profiles for the tails, heads and solvent match well between AA and CG models. However, the CG silicates show a significantly different behavior from their AA counterparts. In the system with anionic silicates (Figure 3, top), these adsorb strongly within the headgroup layer in the AA simulations, while in the CG simulations they are located outside the micelle surface and quite dissolved in the solvent. The differences are even more prominent for the CTAB+SN+H_2O system (Figure 3, bottom), where the CG silicates are completely dissolved in the solvent while the AA silicates again adsorb strongly on the micelle surface. This clearly suggests that the chosen silicate models are too soluble in water. Attempts to describe the

dx.doi.org/10.1021/la3046274 | Langmuir 2013, 29, 2387−2396

silicates using other MARTINI bead types were equally unsuccessful, which indicates that MARTINI 2.0 is not currently able to accurately model silicate molecules in solution.

From our preliminary investigations, it is clear that the position of the silicates relative to the surfactant micelle results from a delicate balance between the electrostatic interaction with the surfactant head (in the case of anionic silicates), the silicate−tail interaction energy and the silicate−solvent interaction energy. We have opted to leave the electrostatic parameters, as well as the size of the beads, unchanged and concentrated on adjusting the other two parameters by trial-and-error until good agreement with the atomistic density profiles was obtained. To reduce the number of adjustable parameters, the silicate-head interaction was also maintained at the original value (ε = 4.5 kJ·mol^{-1}) and we assigned the silicate self-interactions as supra-attractive. Our rationale was to change only interactions involving silicates in order to maintain the correct behavior for CTAB-H_2O solutions (thus the dielectric constant of the medium was kept unchanged), ensure maximum consistency with the original MARTINI force-field (thus the bead size was kept constant), and minimize the degrees of freedom of the model fit (so only the LJ well-depths for silicate−tail and silicate−solvent interactions were changed).

Following the above reasoning, we progressively increased the silicate−tail interaction energy, decreased the silicate−solvent energy, or both. It is important to remark that for each of these interactions we have limited ourselves to the 10 discrete levels of energy prescribed in the MARTINI 2.0 force field.[19] Figures S1−S7 in the Supporting Information qualitatively show the effect of several parameter choices on the micelle density profiles. Generally speaking, when the ratio between ε_{SI-C1} and ε_{SI-P4} is too low, the silicate particles are excessively soluble in water and the silicate peak is more diffuse and located on the outside of the headgroup. Conversely, when this ratio is too high, the silicate density peak moves to the inside of the micelle surface but a significant amount of silica is dissolved inside the hydrophobic core (cf. Figure S2). It is also interesting to note that for some parameter combinations the micelle structure was compromised, and completely unrealistic results were obtained (Figure S3). The best compromise for the interactions between silicates and the other components of the system was obtained by increasing the silicate−tail interaction from 2.0 to 3.5 kJ·mol^{-1} and decreasing the silicate−solvent interaction from 5.6 to 4.5 kJ·mol^{-1}, relative to the original Q_{da} particle. This bead, which we term Q_{SI} (meaning "charged silicate" bead) yields the best quantitative agreement between CG and AA density profiles, as can be seen in Figure 4 (c.f. Figure S4 for a comparison of the four CG models considered for SI), and is thus the proposed model for anionic silicate monomers in this aqueous surfactant solution.

In the case of neutral silicates, we followed the same procedure and a similar effect of the balance between silicate−tail and silicate−solvent interaction was observed (Figures S5−S7). In Figure 5, we can see that the best results were obtained for the new particle type, which we call P_{SN}. It can be seen that the CG silicates are now located inside the micelle headgroup and very close to the AA silicate position, but with negligible solubility inside the hydrophobic core. Interestingly, the values of ε_{SI-C1} and ε_{SI-P4} for the new neutral P_{SN} bead are precisely the same as for the new anionic silicate bead (Q_{SI}) described above, which affords additional physical consistency to our model. For completion, Table 1 shows the interaction

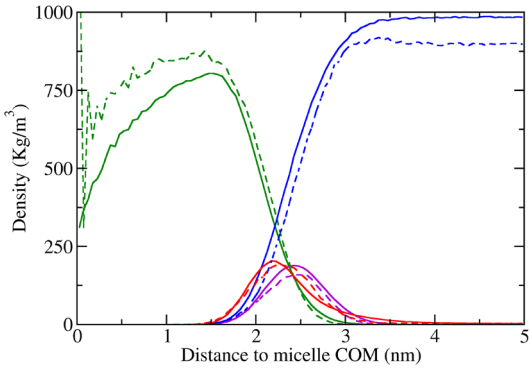

Figure 4. CTA$^+$+SI+H_2O density profiles with a new Q_{SI} CG particle for the ionized silicate. Solid lines represent the AA model, and dashed lines the CG model. Color code is the same as in Figure 3.

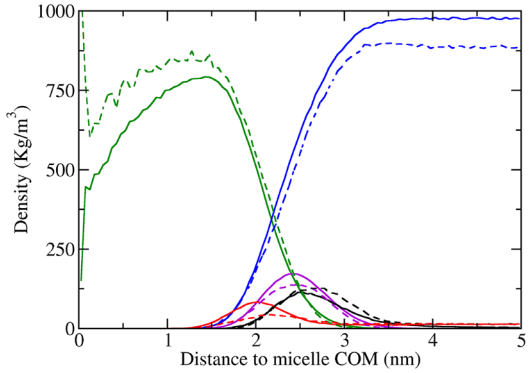

Figure 5. CTAB+SN+H_2O density profiles with a new P_{SN} CG particle for the neutral silicate. Solid lines represent the AA version, and dashed lines the CG one. Color code is the same as in Figure 3.

parameters between both new silicate CG particles and all other components of the system. To summarize this section, a new CG model for silicates in aqueous surfactant solutions has been proposed, thus allowing us to study PMS precursor solutions by long MD simulations, in the range of several microseconds where micelle fusion/fission processes and shape transitions can be explored. This will be the focus of the next section.

3.2. Coarse-Grained Simulations of Self-Assembly in PMS Synthesis Solutions. The coarse-graining procedure as implemented in the MARTINI force field brings about a reduction of the interaction centers in the system by about a factor of 10 (depending on the details of the site mapping) relative to a fully atomistic description, allows for the use of a time step that is about 10 times larger, and speeds up the intrinsic dynamics of the simulation by about a factor of 4.[19,20] Thus, the advantages of CG over AA are a significant reduction in simulation time by about 2 orders of magnitude and in storage requirements by about 1 order of magnitude on average. These advantages are essential for simulating long-chain surfactant molecules like CTAB, and allow us to probe much later stages of silica−surfactant self-assembly than previously accessible using atomistic models.[14,15]

Using the new CG silicate models developed in the previous section, we have carried out long CG simulations for CTAB +H_2O and CTA$^+$+SI+H_2O at two different surfactant concentrations (0.1 and 0.05 M) well above the experimental cmc. Figure 6 shows different instantaneous snapshots taken along the MD simulation for both systems in the case of 0.1 M

dx.doi.org/10.1021/la3046274 | Langmuir 2013, 29, 2387−2396

Table 1. New Lennard–Jones Well-Depth Parameters, ϵ, for Ionized and Neutral CG Silicate Particles[a]

	Q_{SI}	P_{SN}	P_4	BP_4	C_1	Q_0	Q_a
Q_{SI}	5.6(O)		4.5(II)	4.5(II)	3.5(IV)	4.5(II)	
P_{SN}		5.6(O)	4.5(II)	4.5(II)	3.5(IV)	4.5(II)	5.0(I)

[a]The capital letters in parentheses denote the interaction levels according to the standard nomenclature of the MARTINI force-field. In all cases, the value of the LJ site diameter is σ = 0.47 nm. Units of ϵ are kJ/mol.

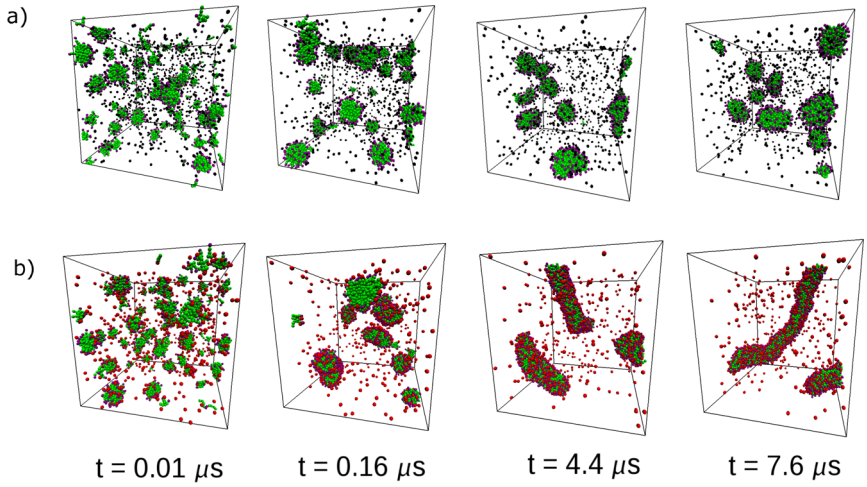

Figure 6. Snapshots of long CG MD simulations for (a) CTAB+H_2O and (b) CTA^++SI+H_2O systems with 0.1 M concentration of surfactant. Color code is green for surfactant tail atoms, purple for surfactant heads, black for bromide ions, and red for anionic silicates (water molecules have been removed for clarity).

concentration of surfactant. The CTAB+H_2O solution is shown in Figure 6a, where we can see how initially small aggregates grow into larger ones to form eight micelles with an average aggregation number of 112, as shown in Table 2. The

Table 2. Results of Long CG Simulations for Aqueous Solutions of Surfactants with or without Silica[a]

system	n	N	R_x	R_y	R_z
CTAB+H_2O (0.1M)	8	112	1.06	1.72	1.90
CTAB+H_2O (0.05M)	8	112	1.04	1.76	1.95
CTA^++SI+H_2O (0.1M)	1	900	19.23	27.15	41.93
CTA^++SI+H_2O (0.05M)	3	300			

[a]Labels n, N, and R_i are used to denote the average number of micelles, number of surfactant molecules in each micelle, and components of the radius of gyration of the micelle, respectively.

formation process of micelles in this class of surfactants has been previously studied in detail by atomistic simulations.[17] The average aggregation number and micelle radius of gyration were obtained by our cluster counting program. The components of the radius of gyration, R_i, also shown in Table 2, point to a prolate ellipsoid shape ($R_x < R_y = R_z$) as observed in atomistic simulations of this class of surfactants[17,18] and in experimental results[44,45,51] for aggregates with more than 90 components. The micelle size for CTAB micelles obtained in this work can be compared to experimental data. One can approximate the micelle radius by the distance between the maximum of the headgroup density profile, colored in purple in Figure 2, and the center of mass of the micelle. The resulting average value was 2.50 nm, which agrees with estimates based on $R = (5R_g/3)^{1/2}$, where R is the radius of an equivalent spherical micelle and R_g is the radius of gyration with $R_g = (R_x^2 + R_y^2 + R_z^2)^{1/2}$. Taking the R_i values for the CTAB+H_2O system in Table 2, we achieve a radius of ∼2.77 nm. These results compare favorably with experimental data in the range of 0.03–0.3 M concentration of surfactant, where values of 2.65 nm,[52] 2.40 nm,[51] and 2.47 nm[46] were reported. In the same way, the aggregation number 112, shown in Table 2 for CTAB+H_2O micelles, is similar to experimental estimates, 104 (0.05 M)[45] and 110 (0.1 M).[51]

A different behavior was obtained for the CTA^++SI+H_2O system where we can observe in Figure 6b the formation of a single rodlike micelle that completely crosses the entire simulation cell. For this system, the second-last row in Table 2 shows one isolated aggregate which contains all the surfactant molecules in the simulation (900). The two smallest components of the radius of gyration, R_x and R_y, are similar, while the third component, R_z, is much larger, which indicates a rodlike structure. The driving force for this sphere-to-rod transition is the strong interaction of anionic silicates with the cationic head groups at the surface of the micelle. This strong adsorption of silicates helps to more effectively screen the repulsion between the cationic head groups of the surfactant, leading to a smaller effective area per headgroup at equilibrium. In other words, upon addition of silica the packing parameter described by Israelachvili[1] is shifting to a value that leads to the formation of aggregates with lower surface curvature, that is, rodlike micelles.

The results obtained with 0.05 M concentration (Figure 7) are quite similar to the 0.1 M results. For CTAB+H_2O at 0.05 M we also obtained eight aggregates with 112 components each on average, as we can see in Table 2. The components R_i of the radius of gyration have similar values to those obtained at 0.1 M, which means that the micelles are also prolate ellipsoids. The last row of Table 2 also shows the results for CTA^++SI+H_2O, where three aggregates with 300 components on average were obtained. We were not able to calculate the values

dx.doi.org/10.1021/la3046274 | Langmuir 2013, 29, 2387–2396

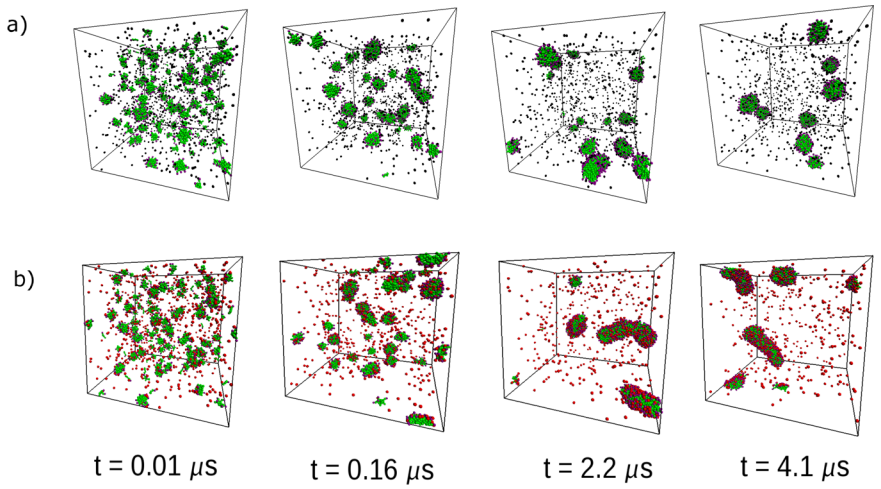

Figure 7. Snapshots of long CG MD simulations for (a) CTAB+H_2O and (b) CTA^++SI+H_2O systems with 0.05 M concentration of surfactant. The simulation time in microseconds is shown for each frame. Color code is the same as in Figure 6.

of the radius of gyration for this particular system since our cluster counting program was not able to handle this kind of configuration. Still, we are currently envisaging a programming strategy in order to solve this problem. Nevertheless, visual inspection of the simulation snapshots (Figure 7b) reveals that the final state for the CTA^++SI+H_2O system is also characterized by rodlike aggregates. It is important to note that our MD production runs for this lower concentration were stopped at 4.1 μs of simulation due to excessive computational requirements (the system is twice as large as the 0.1 M system). It is likely that the CTA^++SI+H_2O system at 0.05 M has not yet completely reached equilibrium, and that given enough time it would evolve to a similar configuration as for the higher concentration, that is, a single rodlike micelle.

If we compare the simulation snapshots shown in Figures 6 and 7, it can be said that the diluted system, 0.05 M, has a slower evolution than at 0.1 M. For example, in the case of the CTA^++SI+H_2O system, the two corresponding snapshots at about 4 μs of simulation time show some differences between the two concentrations. While in the more concentrated solution a large rod is already formed (the three bodies shown in the figure are actually linked through periodic boundary conditions, forming a single aggregate), in the case of the diluted solution we have several micelles in a much earlier stage of the sphere-to-rod transition. This also explains why a single rod is not formed even at 4.1 μs of simulation time for the 0.05 M solution. It is well-known that the so-called second critical micelle concentration, representing the sphere-to-rod transition, is concentration dependent,[41,53−55] which means that this transition occurs earlier in more concentrated solutions, thus corroborating our simulation results.

The sphere-to-rod transition in the CTA^++SI+H_2O 0.1 M simulation takes place very rapidly, which offers an opportunity for us to follow in detail the micelle fusion process leading to rod formation. The snapshots presented in Figure 8 show in cross section how two rather large intermediate-sized micelles merge to form a rodlike aggregate. The two initial micelles have sizes of about 130 surfactants each and have an elongated ellipsoidal shape. To further illustrate the rod-formation process, we have made available a video of the micelle fusion event in the Supporting Information. It can be seen that the two micelles remain close together for a relatively long time without fusion taking place; in some instances, they make

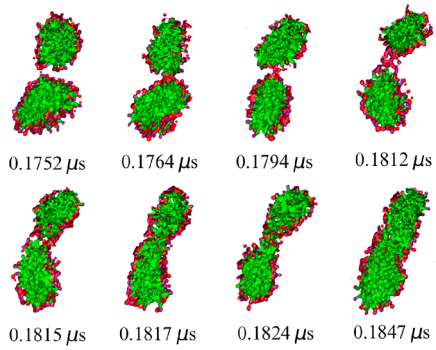

Figure 8. Snapshots for the CTA^++SI+H_2O system with 0.1 M surfactant concentration showing details of the fusion of two spheroidal micelles into a rodlike aggregate. Micelles are shown in cross section to aid visualization. The simulation time in microseconds is shown for each frame. Color code is the same as in Figure 6.

contact (e.g., second frame of Figure 8) but subsequently retreat. Eventually, a rather large bridge is formed between the two aggregates, composed mainly of silicates and charged head groups (fourth frame of Figure 8). Soon after this, tail beads of surfactants belonging to different micelles start to make contact (fifth frame of Figure 8), and the new aggregate quickly equilibrates to a more stable rodlike shape (sixth frame of Figure 8). From this analysis, it appears that the critical step for micelle fusion is the formation of an "ionic bridge" between the two micelles, reinforcing the role of silicates in the sphere-to-rod transition process. The mechanism of sphere-to-rod transition that we observe in our simulations, by fusion of rather large initial micelles, is in agreement with some experimental interpretations,[56−59] but is in contrast to other experimental work suggesting that this transition takes place through successive monomer addition events.[60] In this context, our simulations support recent theoretical studies demonstrating that in many realistic cases, micelle fusion events play an important role in the equilibration of surfactant solutions.[61]

In our previous atomistic study of PMS precursor solutions,[15] we also simulated a system in which silicates were added to a previously equilibrated CTAB+H_2O solution containing small spherical micelles, the so-called "exchange solution". We have replicated this idea with the new coarse-grained model, in order to more faithfully reproduce the real

dx.doi.org/10.1021/la3046274 | Langmuir 2013, 29, 2387−2396

PMS synthesis process. Specifically, we started from an equilibrated configuration of the CTAB+H_2O simulation at 0.1 M concentration of CTAB and randomly added 900 TMASI (tetramethylammonium silicate) ion pairs; that is, the concentrations of surfactant, bromide, silicates, and TMA were all 0.1 M, but the ionic strength of the solution was twice as high as in our original CTA^++SI+H_2O simulation, shown in Figure 6. Tetramethylammonium (TMA) ions were modeled in the MARTINI framework by a single Q_0 bead (i.e., the same as the surfactant headgroup), and the simulation was run for 4 μs after the addition of TMASI. Figure 9 shows the configurations before and after silica addition to the system, while Figure 10 compares the micelle density profiles for those two situations.

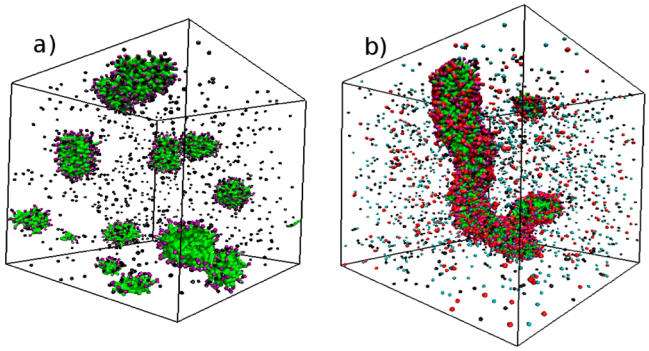

Figure 9. Snapshots for the exchange solution (see text for details). Panel (a) shows the pre-equilibrated CTAB+H_2O micelle solution before the addition of 0.1 M TMASI, and panel (b) shows the final configuration, obtained at 4 μs of simulation time after the addition of silica. Color code is the same as in Figure 6, with the TMA cations represented in cyan.

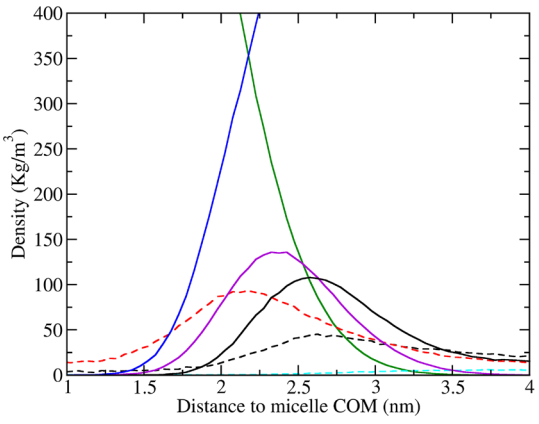

Figure 10. Density profiles for the exchange solution before (full lines) and after (dashed lines) the addition of 0.1 M TMASI. Tail atoms are shown in green, head atoms in purple, water in blue, bromide ions in black, silicates in red, and TMA in cyan. For ease of visualization, tail, head, and water profiles are only shown for the solution without silica.

Our results for the exchange solution clearly show that the behavior is the same as for the solution starting from a random distribution and containing only silicate anions. In fact, the silicates quickly replace the bromide ions at the surface of the micelle, adsorbing once again on the inside of the headgroup region (Figure 10). The bromide peak is significantly reduced relative to the case without silica, indicating that bromide ions are indeed displaced into the bulk solution by the adsorbing anionic silicates. TMA ions are mostly dispersed in the bulk aqueous phase and have negligible effect on the micelle structures. As for the CTA^++SI+H_2O case, the strong adsorption of silicates screens the headgroup repulsion and leads to the formation of rodlike micelles. These simulations clearly show that it is the silicates that are controlling the sphere-to-rod transition in the precursor PMS solutions.

In the silicate solutions discussed above, all silica monomers are anionic (i.e., singly deprotonated). This corresponds to solutions with a very high pH (~14). In reality, PMS synthesis takes place at somewhat lower pH values (around 11[2]), and precursor solutions will be characterized by a distribution of neutral and anionic silicates.[14] To analyze the effect of pH on the micelle evolution, we carried out two simulations analogous to the CTA^++SI+H_2O system but with two different ratios of neutral to anionic monomers: one corresponding to pH = 11 (28 SN and 872 SI molecules), a typical value for PMS synthesis, and another to pH = 9.5 (450 SN and 450 SI), which is equal to the pK_a of monosilicic acid.[62] Snapshots of these three simulations after about 1.4 μs are shown in Figure 11. It is

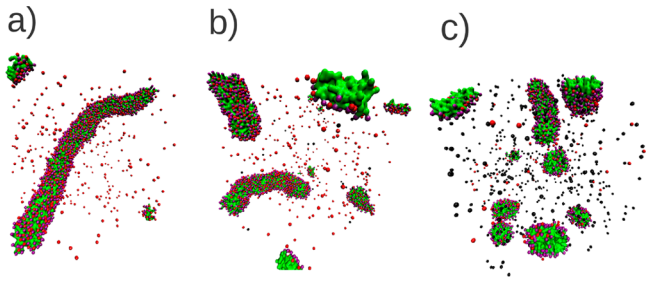

Figure 11. Snapshots for CTAB+SI+SN+H_2O solutions with 0.1 M surfactant concentration at different pH values: (a) pH = 14 (all silicates are ionized); (b) pH = 11 (typical PMS synthesis pH); (c) pH = 9.5 (pK_a of monosilicic acid). For each snapshot, the simulation time is 1.4 μs. Color code is the same as in Figure 6.

clear that at pH = 11, the system behaves in much the same way as the original solution containing only SI; the strong adsorption of anionic silicates leads quickly to rod formation. However, at pH = 9.5, the sphere-to-rod transition appears at least to be slower than that at high pH. This makes physical sense, since the driving force for rod formation is the screening of the repulsive interactions between surfactant head groups by the anionic silicates that adsorb on the micelle surface (see discussion above). At pH = 9.5, even though neutral silicates also adsorb on the micelle surface, the electrostatic screening is not as effective since there are fewer anionic silicates to balance the positive charge of the surfactant heads. Nevertheless, judging by the evolution of the system, it seems likely that complete rod formation would be achieved at longer simulation times.

4. CONCLUSIONS

In this work, we propose a new coarse-grained model for simulating aqueous surfactant solutions containing neutral and anionic silicate molecules. The model was validated by comparing with results of atomistic simulations for preformed spherical micelles. Excellent agreement was observed between AA and CG models for micelle density profiles in all cases. Furthermore, a comparison with experimental data for alkylammonium micelle systems yielded good agreement in essential aspects such as micelle size and shape. This successful validation opens the door to much longer CG simulations in

dx.doi.org/10.1021/la3046274 | Langmuir 2013, 29, 2387−2396

order to explore different stages of aggregation and structural transitions in silica−surfactant solutions.

We have carried out long CTAB+H_2O and CTA^++SI+H_2O CG simulations to study the formation of silica−surfactant mesostructures during the synthesis of periodic mesoporous silica materials. Whereas the solution without silica equilibrated to a distribution of nearly spherical micelles, the solutions containing silica quickly evolved to form rodlike micelles. The sphere-to-rod transition, sparked by the addition of silica to the system, proceeded through the successive fusion of several smaller micelles to form large rods. The driving force for rod formation was seen to be the strong adsorption of anionic silicates on the micelle surface, screening the repulsive interaction between cationic surfactant heads and promoting the formation of structures with lower curvature (i.e., rods). This was shown to be the case either starting from a random initial configuration or by adding silicates to a previously equilibrated solution of CTAB+H_2O composed of nearly spherical micelles. We also analyzed the effect of the solution pH, and showed that at low pH the sphere-to-rod transition is not as favorable, since the relative proportion of anionic silicates is lower. In summary, our simulations demonstrate the ability of silicates to promote a sphere-to-rod transition in surfactant solutions, a crucial step in the templated synthesis of PMS, and thus lend further support to a cooperative mechanism for the formation of this class of materials.

■ ASSOCIATED CONTENT

Ⓢ Supporting Information

Additional figures illustrating the effect of the model parameters on the micelle structure, and video showing the rod formation process in detail. This material is available free of charge via the Internet at http://pubs.acs.org.

■ AUTHOR INFORMATION

Corresponding Author

*E-mail: miguel.jorge@strath.ac.uk.

Notes

The authors declare no competing financial interest.

■ ACKNOWLEDGMENTS

This work is partially supported by projects PEst-C/EQB/LA0020/2011, PEst-C/CTM/LA0011/2011, PTDC/QUI-QUI/109914/2009, and PTDC/EQU-EQU/099423/2008, financed by FEDER through COMPETE - Programa Operacional Factores de Competitividade and by FCT - Fundação para a Ciência e a Tecnologia. M.J. and J.R.B.G. also acknowledge funding from Programa Ciência 2007.

■ REFERENCES

(1) Israelachvili, J. N. *Intermolecular and Surface Forces*; Academic Press: London, UK, 1985.

(2) Beck, J. S.; Vartuli, J. C.; Roth, W. J.; Leonowicz, M. E.; Kresge, C. T.; Schmitt, K. D.; Chu, C. T. W.; Olson, D. H.; Sheppard, E. W.; McCullen, S. B.; Higgins, J. B.; Schlenker, J. L. A New Family of Mesoporous Molecular Sieves Prepared with Liquid Crystal Templates. *J. Am. Chem. Soc.* **1992**, *114*, 10834.

(3) Ying, J. Y.; Mehnert, C. P.; Wong, M. S. Synthesis and Applications of Supramolecular-Templated Mesoporous Materials. *Angew. Chem., Int. Ed.* **1999**, *38*, 56.

(4) Firouzi, A.; Atef, F.; Oertli, A. G.; Stucky, G. D.; Chmelka, B. F. Alkaline Lyotropic Silicate-Surfactant Liquid Crystals. *J. Am. Chem. Soc.* **1997**, *119*, 3596.

(5) Patarin, J.; Lebeau, B.; Zana, R. Recent Advances in the Formation Mechanisms of Organized Mesoporous Materials. *Curr. Opin. Colloid Interface Sci.* **2002**, *7*, 107.

(6) Baute, D.; Frydman, V.; Zimmermann, H.; Kababya, S.; Goldfarb, D. Properties of the Silica Layer during the Formation of MCM-41 Studied by EPR of a Silica-Bound Spin Probe. *J. Phys. Chem. B* **2005**, *109*, 7807.

(7) Bhattacharya, A.; Mahanti, S. D. Self-Assembly of Ionic Surfactants and Formation of Mesostructures. *J. Phys.: Condens. Matter* **2001**, *13*, 1413.

(8) Siperstein, F. R.; Gubbins, K. E. Phase Separation and Liquid Crystal Self-Assembly in Surfactant−Inorganic-Solvent Systems. *Langmuir* **2003**, *19*, 2049.

(9) Gov, N.; Borukhov, I.; Goldfarb, D. Morphological Transitions during the Formation of Templated Mesoporous Materials: Theoretical Modeling. *Langmuir* **2006**, *22*, 605.

(10) Siperstein, F. R.; Gubbins, K. E. Synthesis and Characterization of Templated Mesoporous Materials Using Molecular Simulation. *Mol. Simul.* **2001**, *27*, 339.

(11) Patti, A.; Mackie, A. D.; Siperstein, F. R. Monte Carlo Simulation of Self-Assembled Ordered Hybrid Materials. *Langmuir* **2007**, *23*, 6771.

(12) Patti, A.; Siperstein, F. R.; Mackie, A. D. Phase Behavior of Model Surfactants in the Presence of Hybrid Particles. *J. Phys. Chem. C* **2007**, *111*, 16035.

(13) Schumacher, C.; Gonzalez, J.; Wright, P. A.; Seaton, N. A. Generation of Atomistic Models of Periodic Mesoporous Silica by Kinetic Monte Carlo Simulation of the Synthesis of the Material. *J. Phys. Chem. B* **2006**, *110*, 319.

(14) Jorge, M.; Gomes, J. R. B.; Cordeiro, M. N. D. S; Seaton, N. A. Molecular Simulation of Silica/Surfactant Self-Assembly in the Synthesis of Periodic Mesoporous Silicas. *J. Am. Chem. Soc.* **2007**, *129*, 15414.

(15) Jorge, M.; Gomes, J. R. B.; Cordeiro, M. N. D. S; Seaton, N. A. Molecular Dynamics Simulation of the Early Stages of the Synthesis of Periodic Mesoporous Silica. *J. Phys. Chem. B* **2009**, *113*, 708.

(16) Jorge, M. Structure of Cationic Surfactant Micelles from Molecular Simulations of Self-Assembly. *J. Mol. Struct.: THEOCHEM* **2010**, *946*, 88.

(17) Jorge, M. Molecular Dynamics Simulation of Self-Assembly of *n*-Decyltrimethylammonium Bromide Micelles. *Langmuir* **2008**, *24*, 5714.

(18) Wu, R.; Deng, M.; Kong, B.; Yang, X. Coarse-Grained Molecular Dynamics Simulation of Ammonium Surfactant Self-Assemblies: Micelles and Vesicles. *J. Phys. Chem. B* **2009**, *113*, 15010.

(19) Marrink, S. J; deVries, A. H; Mark, A. E. Coarse Grained Model for Semiquantitative Lipid Simulations. *J. Phys. Chem. B* **2004**, *108*, 750.

(20) Marrink, S. J.; Risselada, H. J.; Yefimov, S.; Tieleman, D. P.; de Vries, A. H. The MARTINI Force Field: Coarse Grained Model for Biomolecular Simulations. *J. Phys. Chem. B* **2007**, *111*, 7812.

(21) Sangwai, A. V.; Sureshkumar, R. Coarse-Grained Molecular Dynamics Simulations of the Sphere to Rod Transition in Surfactant Micelles. *Langmuir* **2011**, *27*, 6628.

(22) Velinova, M.; Sengupta, D.; Tadjer, A. V.; Marrink, S. J. Sphere-to-Rod Transitions of Nonionic Surfactant Micelles in Aqueous Solution Modeled by Molecular Dynamics Simulations. *Langmuir* **2011**, *27*, 14071.

(23) Berendsen, H. J. C.; Van Der Spoel, D.; van Drunen, R. GROMACS: A Message-Passing Parallel Molecular Dynamics Implementation. *Comput. Phys. Commun.* **1995**, *91*, 43.

(24) Lindahl, E.; Hess, B.; Van Der Spoel, D. A Package for Molecular Simulation and Trajectory Analysis. *J. Mol. Model.* **2001**, *7*, 306.

(25) Van der Spoel, D.; Lindahl, E.; Hess, B.; Groenhof, G.; Mark, A. E.; Berendsen, H. J. C. GROMACS: Fast, Flexible and Free. *J. Comput. Chem.* **2005**, *26*, 1701.

(26) Hess, B.; Kutzner, C.; Van Der Spoel, D.; Lindahl, E. GROMACS 4: Algorithms for Highly Efficient, Load-Balanced, and Scalable Molecular Simulation. *J. Chem. Theory Comput.* **2008**, *4*, 435.
(27) Hockney, R. W.; Goel, S. P. J. Quite High Resolution Computer Models of a Plasma. *J. Comput. Phys.* **1974**, *14*, 148.
(28) Bussi, G.; Donadio, D.; Parrinelo, M. Canonical Sampling through Velocity Rescaling. *J. Chem. Phys.* **2007**, *126*, 014101.
(29) Parrinelo, M.; Rahman, A. Polymorphic Transitions in Single Crystals: A New Molecular Dynamics Method. *J. Appl. Phys* **1981**, *52*, 7182.
(30) Berendsen, H. J. C.; Postma, W. F.; van Gunsteren, J. P. M.; DiNola, A.; Haak, J. R. Molecular Dynamics with Coupling to an External Bath. *J. Phys. Chem.* **1984**, *81*, 3684.
(31) Hess, B.; Bekker, H.; Berendsen, H. J. C.; Fraaije, J. G. E. M. LINCS: A Linear Constraint Solver for Molecular Simulations. *J. Comput. Chem.* **1997**, *18*, 1463.
(32) D'Angelo, P.; Migliorati, V.; Guidoni, L. Hydration Properties of the Bromide Aqua Ion: The Interplay of First Principle and Classical Molecular Dynamics, and X-Ray Absorption Spectroscopy. *Inorg. Chem.* **2010**, *49*, 4224.
(33) Berendsen, H. J. C.; Grigera, J. R.; Straatsma, T. P. The Missing Term in Effective Pair Potentials. *J. Phys. Chem.* **1987**, *91*, 6269.
(34) Pereira, J. C. G.; Catlow, C. R. A.; Price, G. D. Ab Inition Studies of Silica-Based Clusters. Part I. Energies and Conformations of Simple Clusters. *J. Phys. Chem. A* **1999**, *103*, 3252.
(35) Pereira, J. C. G.; Catlow, C. R. A.; Price, G. D. Molecular Dynamics Simulation of Methanolic and Ethanolic Silica-Based Sol-Gel Solutions at Ambient Temperature and Pressure. *J. Phys. Chem. A* **2002**, *106*, 130.
(36) Gomes, J. R. B.; Cordeiro, M. N. D. S.; Jorge, M. Gas-Phase Molecular Structure and Energetics of Anionic Silicates. *Geochim. Cosmochim. Acta* **2008**, *72*, 4421.
(37) Olsson, U.; Soderman, O.; Guering, P. Characterization of Micellar Aggregates in Viscoelastic Surfactant Solutions. A Nuclear Magnetic Resonance and light Scattering Study. *J. Phys. Chem.* **1986**, *90*, 5223.
(38) Rao, U. R. K.; Manohar, C.; Valailikar, B. S.; Iyer, R. M. Micellar Chain Model for the origin of Viscoelasticity in Dilute Surfactant Solutions. *J. Phys. Chem.* **1987**, *91*, 3286.
(39) Clausen, T. M.; Vinson, P. K.; Minter, J. R.; Davis, H. T.; Talmon, Y.; Miller, W. G. Viscoelastic Micellar Solutions: Microscopy and Rheology. *J. Phys. Chem.* **1992**, *96*, 474.
(40) Martinez, L.; Andrade, R.; Birgin, E. G.; Martinez, J. M. PACKMOL: A Package for Building Initial Configurations for Molecular Dynamics Simulations. *J. Comput. Chem.* **2009**, *30*, 2157.
(41) Ekwall, P.; Mandell, L.; Solyom, P. The Aqueous Cetyl Trimethylammonium Bromide Solutions. *J. Colloid Interface Sci.* **1971**, *35*, 519.
(42) Atik, S. S.; Thomas, J. K. Photoprocesses in Cationic Microemulsion Systems. *J. Am. Chem. Soc.* **1981**, *103*, 4367.
(43) Lianos, P.; Zana, R. Fluorescence Probe Studies of the Effect of Concentration on the State of Aggregation of Surfactants in Aqueous Solution. *J. Colloid Interface Sci.* **1981**, *84*, 100.
(44) Quirion, F.; Magid, L. J. Growth and Counterion Binding of Cetyltrimethylammonium Bromide Aggregates at 25 °C: A Neutron and light Scattering Study. *J. Phys. Chem.* **1986**, *90*, 5435.
(45) Berr, S.; Jones, R. R. M.; Johnson, J. S., Jr. Effect of Counterion on the size and Charge of Alkyltrimethylammonium Halide Micelles as a Function of Chain Length and Concentration as Determined by Small-Angle Neutron Scattering. *J. Phys. Chem.* **1992**, *96*, 5611.
(46) Hansson, P.; Jonsson, B.; Strom, C.; Soderman, O. Determination of Micellar Aggregation Numbers in Dilute Surfactant Systems with the Fluorescence Quenching Method. *J. Phys. Chem. B* **2000**, *104*, 3496.
(47) Ribeiro, A. C. F.; Lobo, V. M. M.; Valente, A. J. M.; Azevedo, E. F. G.; Miguel, M. G.; Burrows, H. D. Transport Properties of Alkyltrimethylammonium Bromide Surfactants in Aqueous Solutions. *Colloid Polym. Sci.* **2004**, *283*, 277.
(48) Hoshen, J.; Kopelman, R. Percolation and Cluster Distribution. I. Cluster Multiple Labeling Technique and Critical Concentration Algorithm. *Phys. Rev. B* **1976**, *14*, 3438.
(49) Iler, R. K. *The Chemistry of Silica: Solubility, Polymerization, Colloid and Surface Properties, and Biochemistry*; Wiley: New York, 1979.
(50) Hargreaves, R.; Bowron, D. T.; Edler, K. Atomistic Structure of a Micelle in Solution Determined by Wide *Q*-Range Neutron Diffraction. *J. Am. Chem. Soc.* **2011**, *133*, 16524.
(51) Aswal, V. K.; Goyal, P. S. Role of Different Couterions and Size of Micelle in Concentration Dependence Micellar Structure of Ionic Surfactants. *Chem. Phys. Lett.* **2003**, *368*, 59.
(52) Tandford, C. *The Hydrophobic Effect: Formation of Micelles and Biological Membranes*; Wiley, New York, 1980.
(53) Husson, F. R.; Luzatti, V. The Structure of the Micellar Solutions of Some Amphiphilic Compounds in Pure Water as Determined by Absolute Small-Angle X-Ray Scattering Techniques. *J. Phys. Chem.* **1964**, *68*, 3504.
(54) Lindblom, G.; Lindman, B.; Mandell, L. Effect of Micellar Shape and Solubilization on Counter-Ion Binding Studied by 81Br NMR. *J. Colloid Interface Sci.* **1973**, *42*, 400.
(55) Backlund, S.; Holland, H.; Kjammen, O. J.; Ljosland, E. An Ultrasonic Study of Sphere to Rod Transitions in Aqueous Solutions of Hexadecyltrimethylammonium Bromide. *Acta Chem. Scand., Ser. A* **1982**, *36*, 698.
(56) Hayashi, S.; Ikeda, S. Micelle Size and Shape of Sodium Dodecyl Sulfate in Concentrated Sodium Chloride Solutions. *J. Phys. Chem.* **1980**, *84*, 744.
(57) Ozeki, S.; Ikeda, S. The Sphere-Rod Transition of Micelles and the Two-Step Micellization of Dodecyltrimethylammonium Bromide in Aqueous NaBr Solutions. *J. Colloid Interface Sci.* **1982**, *87*, 424.
(58) Ozeki, S.; Ikeda, S. The Sphere-Rod Transition of micelles of dodecyldimethylammonium Bromide in Aqueous Solutions, and the Effects of Counterion Binding on the Micelle Size, Shape and Structure. *Colloid Polym. Sci.* **1984**, *262*, 409.
(59) Ikeda, S. In *Surfactants in Solutions*; Mittal, K. L., Lindman, B., Eds.; Plenum Press: New York, 1984; Vol. *2*; p 825.
(60) Harada, S.; Fujita, N.; Sano, T. Kinetic Studies of the Sphere-Rod Transition of Micelles. *J. Am. Chem. Soc.* **1988**, *110*, 8710.
(61) Griffiths, I. M.; Breward, C. J. W.; Colegate, D. M.; Dellar, P. J.; Howell, P. D.; Bain, C. D. A New Pathway for the Re-Equilibration of Micellar Surfactant Solutions. *Soft Matter* **2013**, *9*, 853−863.
(62) Šefčík, J.; McCormick, A. V. Thermochemistry of Aqueous Silicate Solution Precursors to Ceramics. *AIChE J.* **1997**, *43*, 2773.